A new approach to computing information in measurements of non-resolved space objects by the Falcon Telescope Network

Douglas A. Hope
Department of Physics, USAF Academy
2354 Fairchild Dr., Colorado Springs, CO 80840

ABSTRACT

Space situational awareness (SSA) depends on detection, tracking and characterization of resident space objects. One such system with this capability that is coming online is the Falcon Telescope Network, a network of telescopes dispersed across the state of Colorado as well as around the world. An important capability of the network will be simultaneous observations of a target from multiple sites. Telescopes located in Colorado will enable a study of fast moving low-earth-orbiting targets, while stations around the world will enable study of higher orbiting targets such as those in geosynchronous orbits. Understanding how to exploit this capability to complete tasks related to SSA is analyzed using the framework of statistical information theory. Specific tasks considered include estimating the surface material composition of targets and their intrinsic spin rate. The amount of information in the measurements is computed using simulations of target observations from single and multiple sites in the network. How this approach will lead to optimal use of the network when performing these SSA tasks is presented.

1. INTRODUCTION

A fundamental component of space situational awareness (SSA) is space object identification (SOI). Current SOI methods can be classified as either imaging or non-resolved SOI (NRSOI) [1]. While imaging SOI provides literal images of an object with spatial details, it often requires large aperture telescopes equipped with adaptive optics (AO) systems. NRSOI does not necessarily have such requirements, however, it does require the use of advanced post-processing and analysis algorithms to extract information about the object. Further, in cases where the object is either too small or too distant to be spatially resolved, only NRSOI offers an approach for characterizing the small or distant object. Moreover, NRSOI can be accomplished at a much lower cost because they can use smaller aperture telescopes that do not necessarily require adaptive optics.

In NRSOI the observed photometric signature of a satellite depends on the reflectance properties of its surface materials, its orbital properties, attitude (orientation) and overall shape/physical size. Understanding how each of these factors affects the signature is crucial when extracting any information on the satellite from the data. Current approaches in NRSOI attempt to express the signature as a product function of body and attitude parameters[2], which allows one to make the problem of extracting information a more tractable endeavor. This formalism is well suited for geosynchronous objects where a) the attitude is fixed and often known *a priori* (e.g., the solar panels facing (tracking) the Sun, b) there is general information available on the shape and morphology of the object and c) given their distance from the Earth's surface their orbital position with respect to the Sun and Earth is well characterized by a single parameter, viz., the solar phase angle[3].

NRSOI research on GEO objects has proceeded on essentially two tracks; the first has focused on the problem of their classification based on photometry [4] while the second has focused on the analysis and timing of glints. Particularly, attention has focused on observations during the equinox season where the near zero declination of the sun yields observation conditions such that the solar panels glint thus providing possible information on the shape of the object as seen by the observer [4,5].

Research at AFA focuses on how to use a worldwide network of telescopes to advance current NRSOI capabilities. One such network is the Falcon Telescope Network (FTN) [6], which is a network of commercially available telescopes currently slated to be fully deployed in all hemispheres around[1] the world as shown in Fig. 1.

[1] Telescopes in Vicuna (Chile), La Junta (Colorado-USA) and Canberra (Australia) have been installed and are in the process of becoming operational. Stations in Sardinia, Cape Town and Kauai are in the negotiation phase.

Figure 1 World map showing location of telescopes in Falcon Telescope Network

This arrangement of telescopes gives the ability to simultaneously observe, from multiple sites, space objects in high geosynchronous and semi-synchronous orbits. An arrangement of five telescopes across the state of Colorado[2] (see Fig. 2) offers a similar capability when studying LEO objects.

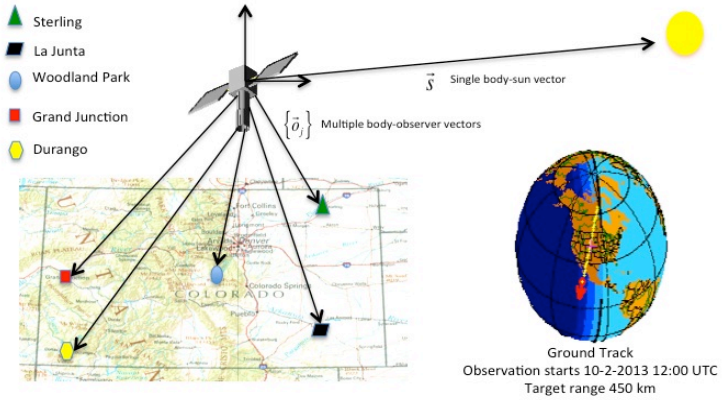

Figure 2 Geographic locations of telescopes in the FTN that reside in Colorado

The research presented here will focus on the problem of studying GEOs when observed simultaneously from multiple sites (La Junta, Colorado and Vicuna, Chile) in different observing modes, broadband measurements using Johnson BVR filters and slitless spectroscopy measurements captured using a diffraction grating. As the effect of this diffraction is to spread the light out into disparate wavelength bands, it should be very applicable to the problem of material identification as each material has a reflectance, which depends on the observation wavelength. Of interest is the comparison of these two observation modes, using both single and multiple sites, in terms of how much information they provide on the surface material composition of a GEO satellite. The framework of statistical information is used for the comparison.

2. OVERVEW OF STATISTICAL INFORMATION

In the context of communication theory, statistical information was defined by Shannon[7], as a measure of information related to uncertainty. Messages with a large amount of uncertainty have a greater potential to convey information than those with a small amount of uncertainty. Mathematically, this is defined in terms of statistical entropy,

$$H(\mathbf{x}) = -\langle \ln p(\mathbf{x}) \rangle \ . \tag{1}$$

[2] Map of Colorado is from the Perry-Castañeda Library Map Collection, University of Texas Library.

where the random vector **x** characterizes a message state. The more 'states' that are accessible by **x**, the larger its entropy and thus greater potential to covey information about the target. The units for information when computed using Eq. (1) are *nats* or natural units due to the use of the natural logarithm. Alternatively, the use of a log-based 2 yields information units of *bits*.

Understanding how the information about a target is captured by FTN observations requires computing the forward observation model $p(\mathbf{m}\,|\,\mathbf{x})$ and the use of Bayes Theorem to obtain the marginal measurement probability function:

$$p(\mathbf{m}) = \int p(\mathbf{m}\,|\,\mathbf{x})p(\mathbf{x})d\mathbf{x} \ . \tag{2}$$

Computing the statistical entropies of $p(\mathbf{x})$, $p(\mathbf{m}\,|\,\mathbf{x})$ and $p(\mathbf{m})$ gives the amount of mutual information (MI) in the FTN measurements

$$\begin{aligned} I(\mathbf{m};\mathbf{x}) &= H(\mathbf{m}) - H(\mathbf{m}\,|\,\mathbf{x}) \\ &= H(\mathbf{x}) - H(\mathbf{x}\,|\,\mathbf{m}) \\ &= H(\mathbf{x}) + H(\mathbf{m}) - H(\mathbf{x},\mathbf{m}) \end{aligned} \tag{3}$$

The MI will depend on the number of stations used to observe the target, the signal to noise ratio (SNR) of the measurements, atmospheric extinction, instrument sensitivity, and finally the particular observing modality.

3. MODELING A GEO-SYNCHRONOUS SATELLITE

Framing the problem of material identification using statistical information requires a GEO satellite to be modeled in a statistical sense. The first assumption for the model is that the satellite is attitude stabilized and has the shape of a rectangular facet with a length and width on the order of 32 meters and 3m respectively. The surface materials on this facet are modeled as an areal mixture of five different distinct materials. The fractional abundances (FA) of each material in the mixture are represented by the components of the random variable **x,** with their respective mean abundance summarized in the table in Fig. 3. Here, each material configuration denoted by **x** represents a state of the system (GEO model), and thus the mean and uncertainty on the components of **x** represent our prior statistical information about the surface materials on the GEO. In the modeling done here a total of 512 different material configurations were considered in the model.

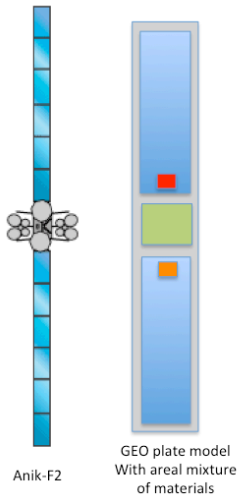

Material	Material Description	Fractional Abundance Mean value
1	TASAT BRDF# MB 0023 Solar Cell, Silicon, Sun Side	0.80
2	TASAT BRDF# MB 0001 Aluminum Alloy, 2024-T3, Polished	0.07 +/- 0.007
3	TASAT BRDF# MB 0026 Kapton, Aluminized 1 Mil, Kapton Side out	0.05 +/- 0.005
4	TASAT BRDF# MB 0029 Mylar, Aluminized, Mylar Side	0.05 +/- 0.005
5	TASAT BRDF# MB 0061 Paint, Chemglaze Z202, White	0.05 +/- 0.005

Figure 3 A statistical model of a GEO satellite with the FA of surface materials in the table modeled using a Gaussian distribution

For each realization of a GEO, the brightness of the reflected sunlight has been computed using a method similar to that in the AFRL Time-Domain Analysis Simulation for Advanced Tracking (TASAT) satellite modeling tool [8,9]. The method uses the bi-reflectance distribution functions (BRDF), in particular the Maxwell-Beard BRDF [10,11]. The primary material on the satellite is MB 0023 – Solar Cell, Silicon, Sun Side and on average contributes to 80% of the total surface area of the GEO. The secondary materials and their average fractional abundances are Aluminum (0.07 +/- 0.07), Kapton (0.05+/- 0.05), Mylar (0.05+/-0.05) and White paint (0.05+/-0.05).

In the statistical model of the GEO a particular material configuration is characterized by a Gaussian random vector $\mathbf{x}=(x_1,x_2,x_3,x_4)$, where the components denote the FA for each of the secondary materials. The abundance of the solar cell material on a particular realization of the GEO is $1 - (x_1 + x_2 + x_3 + x_4)$. In our GEO model the albedo-area product is held fixed over the wavelength range of interest, and as a consequence statistical fluctuations of the FA in our model result in variations in the physical size (area) of the GEO. In other words, the statistical model includes the possible realizations of a GEO with material mixtures and physical sizes that correspond to a fixed value of the albedo-area product.

In this work a total of 512 distinct material configurations on the GEO has been considered. Each configuration contributes to the statistical entropy in Eq. (1) yielding a total of 9 bits of information. The flux distribution of the GEO ensemble as a function wavelength is plotted on the left in Fig. 4. As the solar cell material is the primary material on the target (at approximately 80% of the surface area), the mean values of the flux distribution at each wavelength represent the reflectance of solar cell material. Overall, the GEO statistical model has a reflectance of solar cell (MB 0023) with fluctuations about this mean resulting from statistical fluctuations in the FA. At short wavelengths (0.4 microns) there is a large scatter in the distribution of flux, which corresponds to a larger statistical entropy as shown on the right (blue squares). At 0.60 microns, there is a noticeable sharpening in the distribution and thus lower entropy. At longer wavelengths (beyond 0.70 microns) this distribution begins to broaden and thus the statistical entropy begins to increase again (red circles). As the statistical entropy represents a *global* characteristic of a probability distribution, the plots on the right provide insight on how many realizations are required to fully characterize the GEO, as shown in Fig 3 in a statistical fashion. Convergence of $H(X)\big|_\lambda$ to a constant value (after about 400 realizations) indicates the statistics are being properly characterized.

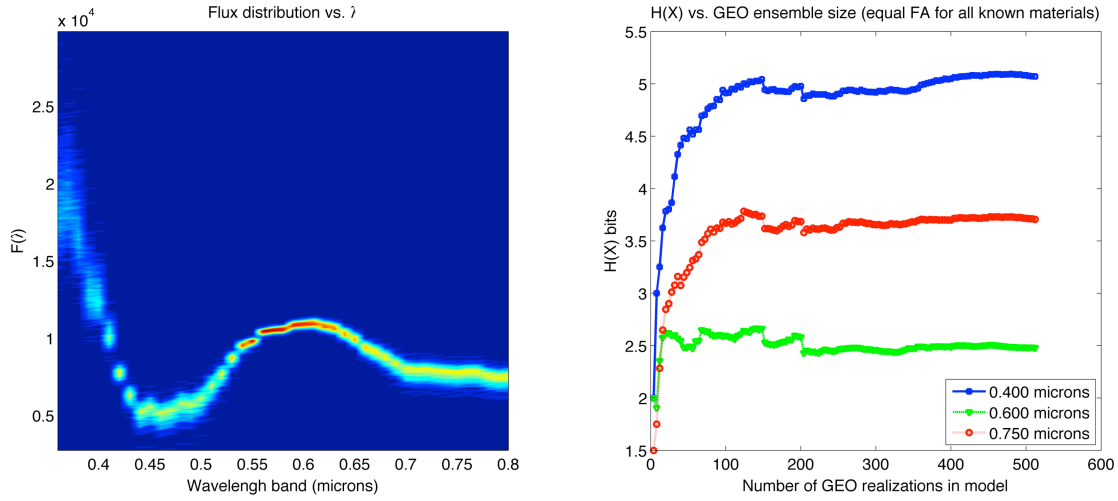

Figure 4 Left: The flux distribution of the GEO ensemble as a function of wavelength bin. On the right are the statistical entropies of the flux distributions at 0.40, 0.60 and 0.75 microns.

4. MUTUAL INFORMATION IN GEO OBSERVATIONS

For each material configuration in the GEO ensemble, an observed brightness is generated by propagating the orbital parameters in the TLE (Anik-F2 SSN 28378) for a 1.5-hour observation during the 2013 spring equinox prior to and during the glinting of the solar panels. As a function of wavelength, the GEO brightness m_λ is generated in time

increments of 30 seconds at wavelength increments of 10nm over the range of 400-800nm, which covers the bandwidth of the Johnson BVR filters. The flux density is $F_{obj} = F_{sun} 10^{0.4 m_v} (1.944e-11)$ where F_{sun} is based on the ASTM E-490 spectrum [12]. The observed photon flux[13] is

$$K_\lambda = \frac{F_{obj} A \tau \Delta\lambda \Delta t}{hc/\lambda} \tag{4}$$

where A is the aperture area (0.5m), $\Delta\lambda$ is the bandwidth (10nm), τ is the atmospheric transmission (assumed to be 0.5), Δt is the integration time, h is Planck's constant, c is the velocity of light and λ is the imaging wavelength [6].

The MI is related to how well the uncertainty in the FA of surface materials (characterized by the GEO ensemble) is preserved in the measured data. A successful measurement strategy should convey most, if not all, of the uncertainty (entropy). Thus, we interpret the MI as a measure of the potential for the measurements to convey information about the amount of each principal materials on the object.

Two measurement strategies that are considered here are broadband and spectroscopic measurements of a GEO satellite. Of interest is how much information is captured by broadband and spectroscopic measurements as the object moves through zero solar phase angle. For the broadband measurement scenario the BVR filters have been considered, where each filter corresponds to a wavelength bin.

There are some challenges when observing GEOs during a glint season as the brightness can increase several orders of magnitude over the night. As a consequence, the exposure time will need to decrease as the object begins to glint in order to avoid any non-linear effects and/or detector saturation. To overcome this problem, the exposure time is continually adjusted so as to achieve a constant, but acceptable signal-to-noise ratio (SNR) value. This allows us to interpret the resultant changes in MI throughout the night as being dependent on the illumination geometry, which changes as the Earth rotates.

Computing the MI requires an appropriate noise model to generate the measurement probability function. To accomplish this we modeled the noise as a zero mean Gaussian with σ_N. During glint at time t, for an observation performed simultaneously in different wavelength bands and from different sites, the conditional measurement probability function is,

$$p(\mathbf{m} \mid \mathbf{x}) = \prod_s \prod_w \frac{1}{\left(2\pi\sigma_N\right)^{1/2}} \exp\left[\frac{-\left\|\mathbf{m} - K_{sw}(\mathbf{x})\right\|^2}{2\sigma_N^2}\right]$$

where the subscripts s and w index the FTN site and wavelength bin/filter. The mean flux value for *w-th* wavelength bin at site *s,* where the width of the wavelength bin is $\Delta\lambda$ with central wavelength of λ, is computed via Eq. (4).

Computing the statistical entropy of the measurement probability function requires first evaluating the integral in Eq. (2). This is done using the Metropolis-Hastings Monte Carlo method [14], which creates a sequence of random values that approximately follows the distribution p(**m**). The algorithm starts with some initial measurement value $\mathbf{m}_{i=0}$ for the sequence, the proposed next measurement value in the sequence is drawn according to a proposal distribution, taken to be a Gaussian here. The value of the ratio a=P($\mathbf{m}_{i+1}$)/ P($\mathbf{m}_i$) determines whether the proposed value is included in the sequence, for a >= 1 it is accepted and for a<1 it is accepted with probability of p*(1-a)*. The algorithm is allowed to iterate until some convergence is achieved, such that the statistics of the sequence follow the distribution p(**m**).

One challenge when using this method is the multi-modal nature of the measurement probability function p(**m**) as demonstrated in Fig 5 for the case of a two channel BV-filter measurement scenario. On the left is a histogram evaluation of p(**m**) where each pixel in the histogram corresponds to **m** = (m_1, m_2) with m_1 = B-flux and m_2 = V-flux both in photons. The middle plot denotes the mean B and V flux values for each of the 512 realizations in the GEO

model. The final plot on the right demonstrates the MC sequence of random variables (measurements) {**m***} used to compute the statistical entropy of p(**m**) which is $H(\mathbf{m}) \approx -\left\langle \log_2 p(\mathbf{m}^*) \right\rangle$. The MI in the measurements is computed via Eq. (3).

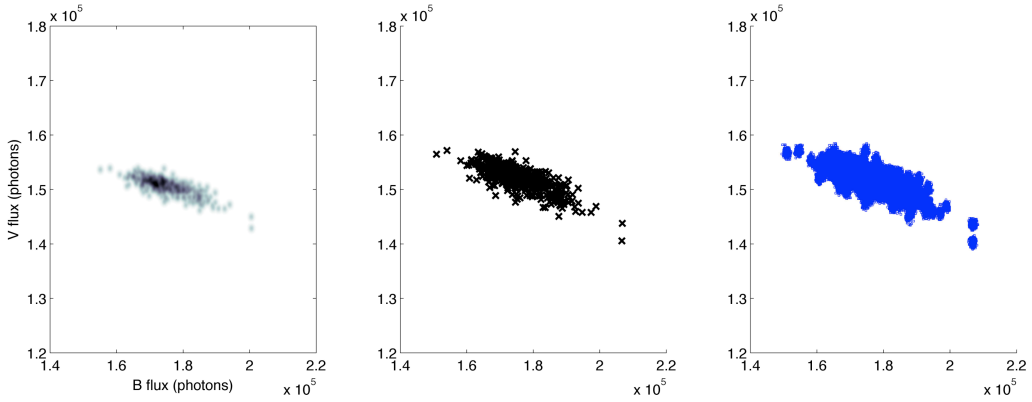

Figure 5 Left: Measurement probability function evaluated for a 2-channel (B and V) measurement evaluated using a histogram. The middle plot shows the mean values of the B-flux and V-flux for each of the 512 realizations in the GEO model. The right plot shows the steps for each of the 512 Monte-Carlo samplers (centered on the mean values) after 500 iterations.

The problem of the multimodal distribution is overcome by running an independent sampler at each mean value [14]. As there are 512 realizations in the GEO model, there are 512 independent Monte Carlo samplers being run. The sequence for p(**m**) is updated at each iteration by including the contribution of these independent samplers.

Of interest here is how broadband and spectroscopic measurements capture information about the surface materials on the GEO. Single measurements using the B,V and R filters capture photons over a fairly large spectral bandwidth, typically 100-150nm, while measurements using the slitless spectroscopy capture photons in much smaller wavelength bins, with the bin size depending on the diffraction grating. The effect of this is an increase in discrimination ability amongst the different surface materials, as each material has a reflectance with certain wavelength dependence. However, associated with this increase in spectral resolution is a subsequent decrease in the number of photons per wavelength bin, which leads to a lower SNR.

In addition to comparing the tradeoff between broadband and spectroscopic measurements, there is the question of how multisite observation capabilities of the FTN might provide more information than just single site observations alone. Figure 6 summarizes the MI in broadband and slitless spectroscopy measurements when a GEO is observed from a single site or two sites (LaJunta, CO and Vicuna, Chile) near glint. The blue squares, green triangles and red circles denote the single B,V, and R filter measurements. The B-band captures the most information about the object (about 30%), while the V-band captures the least information (about 20%). Most likely this results from the lower reflectivity solar cell material (on average 80% of the surface area) at the visible wavelengths,

Next, the MI captured by broadband BVR observations from a single site (Colorado or Chile) is plotted; where it was assumed that the object was simultaneously observed through all three filters. In practice it may be possible to perform these measurements sequentially, depending on the temporal resolution needed to resolve glint features. The MI in joint broadband measurements using both Chile and Colorado is about 6 bits of information.

Finally, the MI captured by the spectroscopic measurements is plotted for a single Colorado site and a joint measurement between Colorado and Chile. In both cases, the peak MI in the measurements occurs for about 5 spectral bins, which implies that these measurements should capture the most information on the FA of materials. A joint measurement using five spectral bins captures almost 8 bits of information or about 88% of the total information on the materials in our GEO model.

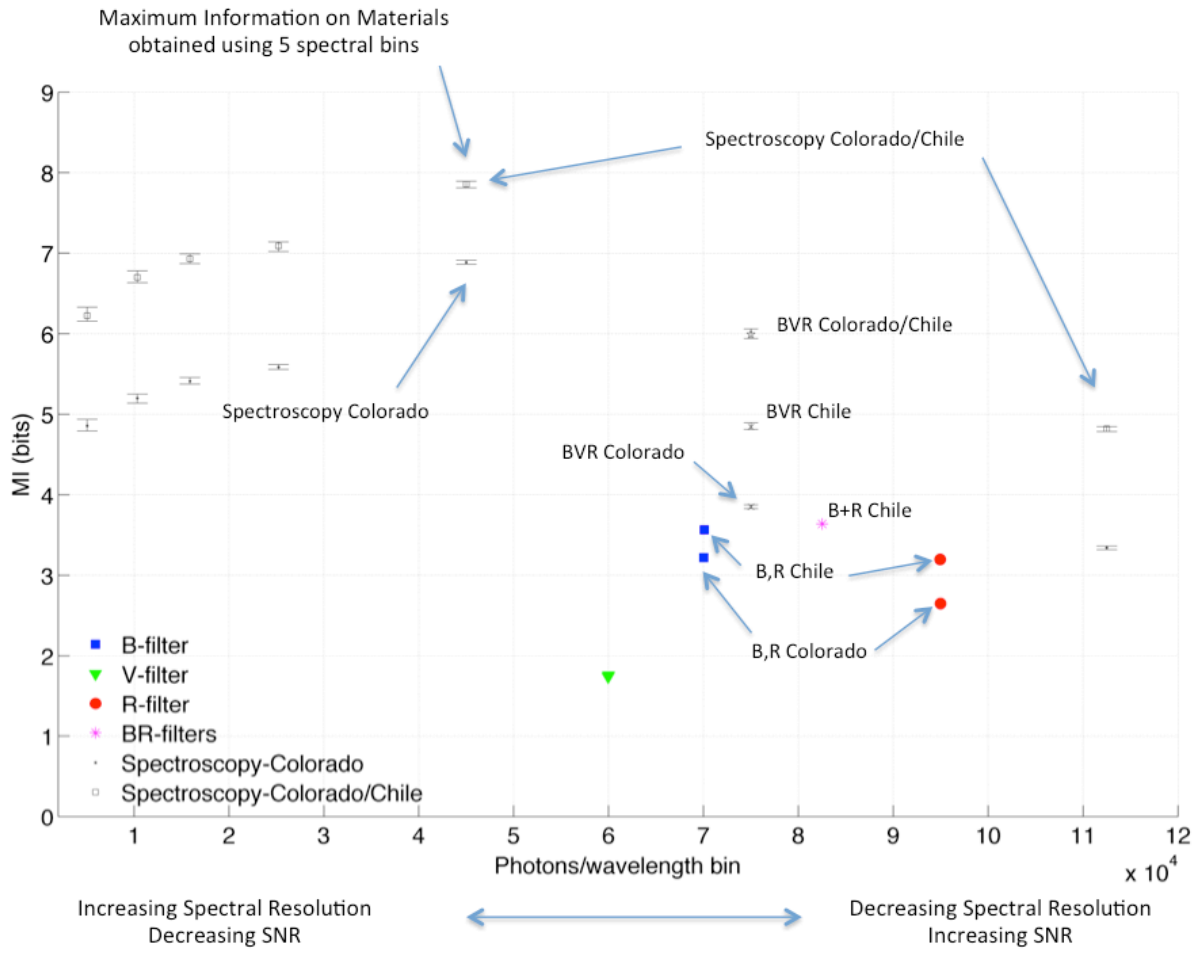

5. CONCLUSIONS

The MI analysis of broadband and spectroscopy observing modes of the FTN show the advantages of using spectroscopic measurements over simple broadband measurements. Insight on how to chose the diffraction grating has been gained and the advantage of joint multi-site measurements has been demonstrated.

Future research will address the question of how does averaging the slitless-spectroscopy measurements increase information, as such an approach should reduce the noise and thus allow one to leverage a higher spectral resolution (greater material discrimination) than just five bins. Likewise, the averaging could be applied to broadband measurements, but it is not clear how a reduction in noise would increase the MI as the spectral resolution is essentially fixed by the bandwidth of the individual B,V, and R filters. Further, the time over which the measurement averaging is done will be determined by the desired temporal resolution required to detect glints from surface features on the GEO.

The analysis here has focused on the case when the surface materials are know, but the FA are unknown and must be estimated. One constraint on the FA was that the solar cell material comprised on average 80% of the GEO surface area. An extension of this work would be to the problem when the surface materials on the GEO are not well known, as when studying a GEO where no manufacturing data is available (e.g., a satellite launched and operated from a different country). Here, uncertainty in the principal materials would be included in the GEO model.

6. ACKNOWLEDGEMENT

Research supported by AFOSR funding via the USAFA-AFOSR MOA dated Oct 2013

7. REFERENCES

[1] Lambert, J. and Kissel, K., "The Early Development of Satellite Characterization Capabilities at the Air Force Laboratories", The 2006 AMOS Technical Conference Proceedings, Kihei, HI, 2006.

[2] Hall, D. "Separating Attitude and Shape Effects for Non-resolved Objects", The 2007 AMOS Technical Conference Proceedings, Kihei, HI, 2007.

[3] Kervin, P., Hall, D. and Bolden, M., "Phase Angle: What is it Good For", The 2010 AMOS Technical Conference Proceedings, Kihei, HI, 2010.

[4] Payne, T,. et al., "SSA Analysis of GEO Photometric Signature Classifications and Solar Panel Offsets", The 2006 AMOS Technical Conference Proceedings, Kihei, HI, 2006.

[5] Hall, D. and Kervin, P., "Analysis of Faint Glints from Stabilized GEO Satellites", The 2013 AMOS Technical Conference Proceedings, Kihei, HI, 2013.

[6] Dearborn, M., et al., "USAF Academy Center for Space Situational Awareness", The 2012 AMOS Technical Conference Proceedings, Kihei, HI, 2012.

[7] Shannon, C., The Bell System Technical Journal,Vol. 27, pp. 379-423, 623-656, July, October, 1948.

[8] F. Riker et al., "Satellite Imaging Experiment tracking simulation results," Proc. SPIE Vol. 2221, 235-247 (1994)

[9] Maxwell, J.R., Beard, J., et.al., ―Bi-directional Reflectance Model Validation and Utilization, *Air Force Avionics Laboratory Technical Report*, AFAL-TR-73-303, October 1973.

[10] Hall, D., "Optical CubeSat Discrimination", The 2008 AMOS Technical Conference Proceedings, Kihei, HI, 2008.

[11] Hall, D., "Surface Material Characterization from Multi-band Optical Observations", The 2010 AMOS Technical Conference Proceedings, Kihei, HI, 2010.

[12] 2000 ASTM Standard Extraterrestrial Spectrum Reference E-490-00

[13] S. R. Maethner, Deconvolution from wave-front sensing using optimal wave-front estimators, Thesis, Air Force Institute of Technology, AFIT/GSO/ENP/96D–01, p 42–43 (1996)

[14] N. Metropolis, A.W. Rosenbluth, M.N. Rosenbluth, A.H. Teller, E. Teller, "Equations of State Calculations by Fast Computing Machines," Journal of Chemical Physics, vol. 21 (6), pp. 1087 1092. (1953)

[15]. Prasad, S. *private conversation*, at the AFOSR 2013 Spring Review, Albuquerque NM